PERIODICO di MINERALOGIA
established in 1930

Dipartimento di Scienze della Terra
Sapienza Università di Roma

An International Journal of
Mineralogy, Crystallography, Geochemistry,
Ore Deposits, Petrology, Volcanology
and applied topics on Environment, Archaeometry and Cultural Heritage

Crystal-chemistry of sulfates from Apuan Alps (Tuscany, Italy). I. Crystal structure and hydrogen bond system of melanterite, $Fe(H_2O)_6(SO_4)\cdot H_2O$

Daniela Mauro, Cristian Biagioni *, Marco Pasero

Department of Earth Sciences, University of Pisa, Via Santa Maria 53, 56126 Pisa, Italy

ARTICLE INFO

Submitted: July 2017
Accepted: November 2017
Available on line: January 2018

* Corresponding author:
cristian.biagioni@unipi.it

DOI: 10.2451/2018PM759

How to cite this article:
Mauro D. et al. (2018)
Period. Mineral. 87, 89-96

ABSTRACT

Melanterite, ideally $Fe(H_2O)_6SO_4\cdot H_2O$, from the pyrite+iron oxide ore deposit of Fornovolasco (Apuan Alps, Tuscany, Italy) has been fully characterized through electron microprobe analysis, micro-Raman spectroscopy, and X-ray diffraction. Melanterite occurs as cm-sized greenish fibrous efflorescences on pyrite or rare pseudo-octahedral colorless crystals, up to 5 mm in size. Electron microprobe analysis (in wt% - average of ten spot analyses normalized to 100 wt% without H_2O) gave: SO_3 52.98, FeO 45.53, MgO 1.49, sum 100.00. Assuming the occurrence of 7 H_2O groups per formula unit, the chemical formula can be written as $(Fe_{0.95}Mg_{0.06})_{\Sigma 1.01}(SO_4)\cdot 7H_2O$. The Raman spectrum of melanterite is characterized by bending and stretching modes of (SO_4) and H_2O groups. Melanterite crystallizes in the space group $P2_1/c$, with unit-cell parameters a=14.0751(8), b=6.5014(4), c=11.0426(6) Å, β=105.632(3)°, V=973.11(10) Å^3, Z=4. The crystal structure of melanterite refined to R_1 = 0.024 on the basis of 3457 unique reflections with $F_o>4\sigma(F_o)$ and 179 refined parameters. It can be described as formed by undulating layers showing the alternation, along **a**, of SO_4 groups and Fe-centered octahedra coordinated by H_2O groups. The occurrence of a complex hydrogen bond system plays a fundamental role in the crystal structure of melanterite.

Keywords: melanterite; sulfate; crystal structure; hydrogen bonds; Fornovolasco; Apuan Alps.

INTRODUCTION

Melanterite is the eponymous mineral of a group of natural and synthetic compounds having general formula $M^{2+}SO_4\cdot 7H_2O$, where M represents a divalent cation such as Co, Cu, Fe, Mg, Mn, and Zn (Peterson, 2003). Melanterite is one of the first products of the interaction between sulfide mine-waste and water at relatively high humidity conditions (e.g., Frau, 2000). The crystal structure of its syntethic analogue was first solved by Baur (1964) based on film data, and later refined by Fronczek et al. (2001) on the basis of CCD data. Peterson (2003) examined both synthetic and natural samples of melanterite, pointing out the relationships between the structural distortion and the Cu content. Hydrogen positions were not reported by this author. A description of the hydrogen bonding in melanterite was provided by Anderson et al. (2007) who refined the crystal structure of synthetic deuterated heptahydrate ferrous iron sulfate on the basis of neutron powder-diffraction data. However, as stated by these authors, a shortcoming of the neutron diffraction on a deuterated sample is that the scattering is dominated by deuterium (D), thus resulting in a lower accuracy in the determination of non-D atoms.

The occurrence of sulfates related to the weathering of the pyrite±baryte±iron oxide ore deposits from Apuan Alps has been known since D'Achiardi (1872). Recently,

Biagioni et al. (2011) reported the presence of sulfate assemblages originating from the alteration of pyrite in the old tunnels of the Fornovolasco mine, Fabbriche di Vergemoli, Lucca. The occurrence of well-crystallized sulfates made these samples suitable for single-crystal X-ray diffraction studies; moreover, the peculiar geochemistry of the pyrite ores, particularly enriched in Tl (up to 1100 µg/g - D'Orazio et al., 2017), made relevant the full-characterization of the sulfate assemblages from an environmental perspective. The first oxidation and hydration product of pyrite is represented by melanterite occurring either in sulfate piles or as efflorescence on the tunnel walls where the pyrite ore bodies are exposed (Figure1a).

The availability of well-crystallized natural samples allowed the structural investigation of melanterite and its H-bond system, overcoming the weakness of the previous structural determinations (e.g., the relatively low accuracy in the determination of non-D atoms by Anderson et al., 2007). Therefore, the aim of this study is the description of the H-bond system based on the crystallographic examination of melanterite from Fornovolasco, comparing these results with those previously achieved on synthetic analogs.

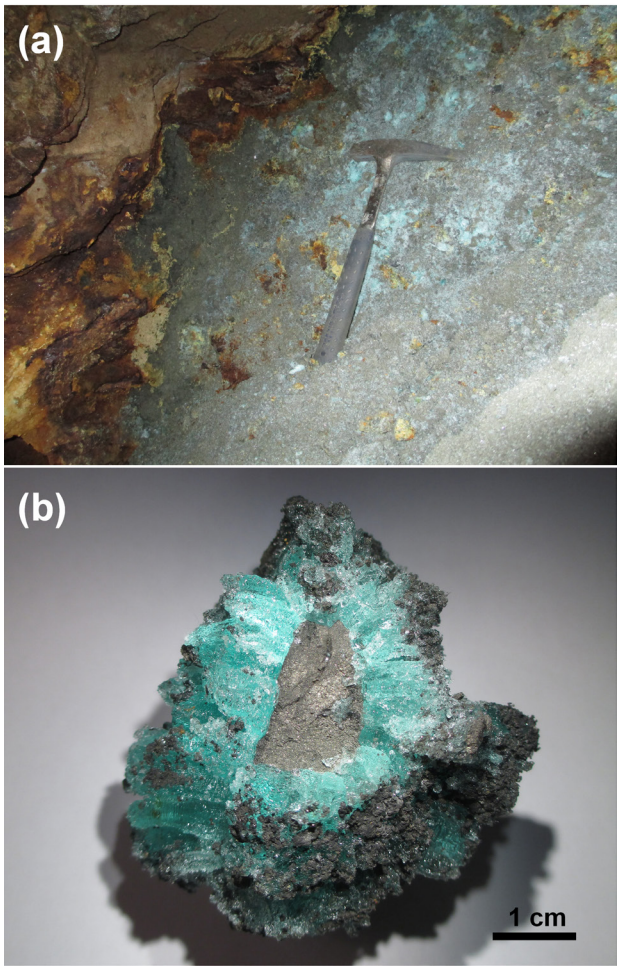

Figure 1. Melanterite from Fornovolasco (Apuan Alps, Tuscany, Italy), as efflorescence on the pyrite masses exposed in the old tunnels (a), and as beard-like aggregates formed around a core of microcrystalline pyrite (b).

EXPERIMENTAL

The studied specimen of melanterite was collected in the old tunnels of the pyrite-iron oxide mine of Fornovolasco (Fabbriche di Vergemoli, Apuan Alps, Tuscany, Italy). Melanterite occurs as greenish beard-like fibrous aggregates (Figure1b), up to 1 cm in size, associated with pyrite and minor römerite. Equidimensional, anhedral crystals and rare pseudo-octahedral crystals, due to equal development of {110}, {001}, and {$\bar{1}$01} faces, have been observed.

Chemical data

Preliminary qualitative chemical analyses were performed using a Philips XL30 scanning electron microscope equipped with an EDAX DX-4 system operating in energy dispersive mode. Iron and S were found as the only elements with Z>8 above the detection limit. Quantitative chemical data were collected through a Superprobe JEOL JXA 8200 electron microprobe at the "Eugen F. Stumpfl" laboratory, Leoben University, Austria, using the following analytical conditions: WDS mode, accelerating voltage 10 kV, beam current 10 nA. The beam size was set to 20 µm in order to minimize the sample damage. The following standards (element, emission line) were used: magnetite (Fe*K*α), olivine (Mg*K*α), and NiS (S*K*α). The ZAF routine was applied for the correction of the recorded raw data. Counting times were 15 s for peak and 5 s for backgrounds. Electron microprobe analysis of melanterite is very difficult as fluid inclusions burst because of both the vacuum and the heating by the electron beam (e.g., Peterson, 2003). In this way, the carbon coating and the polished surface are rapidly destroyed. Moreover, the heating favors the dehydration of melanterite. To account for these inconveniences, the analytical total, without H_2O, was normalized to 100.00 wt%. The following results were obtained (in wt% - average of 10 spot analyses): SO_3 52.98(1.03), FeO 45.53(1.11), and MgO 1.49(31). On the basis of 4 O atoms per formula unit, assuming the occurrence of 7 H_2O, in agreement with the crystal structure refinement, the chemical formula of melanterite from Fornovolasco could be written as $[Fe_{0.95(3)}Mg_{0.06(1)}]_{\Sigma 1.01(3)}S_{1.00(1)}O_4 \cdot 7H_2O$. The occurrence of minor Mg in melanterite agrees with the existence of the Mg-analog of melanterite, i.e. alpersite (Peterson et al., 2006).

Micro-Raman spectroscopy

Unpolarized micro-Raman spectra were collected on unpolished samples of melanterite in nearly backscattered geometry with a Jobin-Yvon Horiba XploRA Plus apparatus, equipped with a motorized *x*-*y* stage and an Olympus BX41 microscope with a 10× objective. The Raman spectra were excited using a 532 nm line of a solid-state laser attenuated to 25% in order to minimize the sample damage. The minimum lateral and depth resolution was set to a few micrometers. The system was calibrated using the 520.6 cm^{-1} Raman band of silicon before each experimental session. Spectra were collected through multiple acquisitions with single counting times of 60 s. Backscattered radiation was analyzed with a 1200 mm^{-1} grating monochromator.

The Raman spectrum of melanterite, shown in Figure 2, can be divided into three regions, i.e. between (i) 200-1200 cm^{-1}, (ii) 1400-1800 cm^{-1}, and (iii) 3000-3600 cm^{-1}.

The region between 200 and 1200 cm^{-1} (Figure 2a) is dominated by bands arising from the (SO_4) group vibrations. The most strong band occurs at 981 cm^{-1} and can be interpreted as due to the symmetrical stretching ν_1 of the (SO_4) group. Its position agrees with those reported by previous authors (e.g., Chio et al., 2005; Sobron and Alpers, 2013). Moreover, Chio et al. (2005) observed that this band position is related to the hydration state of the iron sulfates; in the studied sample it agrees with the heptahydrate nature. Two weaker bands at 1102 and 1144 cm^{-1} can be assigned to the antisymmetrical stretching mode ν_3 of the (SO_4) group. These positions are comparable with those reported by Chio et al. (2005), i.e. 1102 and 1139 cm^{-1}.

The bending modes of the (SO_4) group are represented by bands at 456 (ν_2 mode) and 605 cm^{-1} (ν_4 mode). A weak band at 380 cm^{-1} has been interpreted to a vibration of the $[Fe(H_2O)_6]^{2+}$ complex (e.g., Sobron and Alpers, 2013). The band at 242 cm^{-1} can be attributed to Fe-O vibration modes. The occurrence of H_2O groups is confirmed by the occurrence of bending and stretching vibrations of O-H bonds. The former are represented by a weak band centered at 1656 cm^{-1} (Figure 2b), whereas the latter are represented by a broad and intense band, as typical of several hydrated iron sulfates. Two maxima can be identified, at 3244 and 3429 cm^{-1} (Figure 2c), in agreement with the values reported by Chio et al. (2005), i.e. 3245 and 3427 cm^{-1}. The shape and the broad continuum of such a band is determined by the convolution of several vibrational modes of non-equivalent O-H bonds.

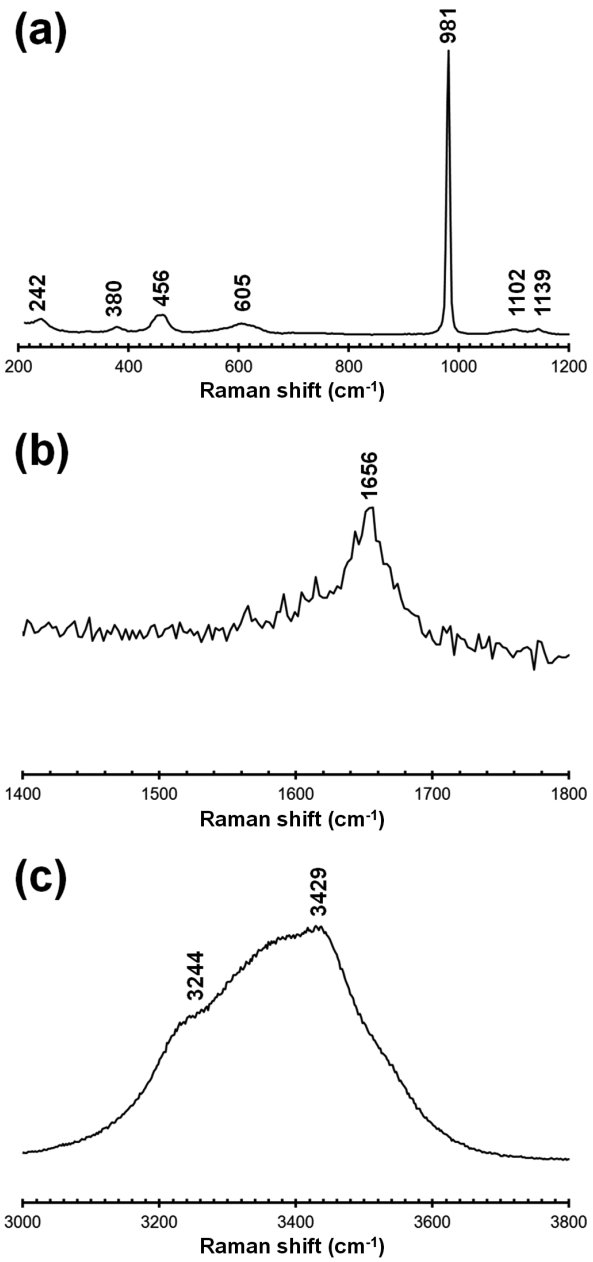

Figure 2. Micro-Raman spectrum of melanterite in the regions between 200-1200 cm^{-1} (a), 1400-1800 cm^{-1} (b), and 3000-3800 cm^{-1} (c).

X-ray crystallography

Intensity data were collected using a Bruker Smart Breeze diffractometer operating at 50 kV and 30 mA and equipped with an air-cooled CCD detector. Graphite-monochromatized Mo$K\alpha$ radiation was used. The detector-to-crystal working distance was set to 50 mm. A total of 1642 frames were collected using φ and ω scan modes, with an exposure time of 5 seconds per frame. Intensity data were integrated and corrected for Lorentz, polarization, background effects, and absorption using the package of software APEX 2 (Bruker AXS Inc., 2004). The statistical tests on the distribution of $|E|$ values

Table 1. Crystal data and summary of parameters describing data collection and refinement for melanterite.

Crystal data	
Crystal size (mm)	0.13 × 0.08 × 0.08
Cell setting, space group	Monoclinic, $P2_1/c$
a (Å)	14.0751(8)
b (Å)	6.5014(4)
c (Å)	11.0426(6)
β (°)	105.632(3)
V (Å^3)	973.11(10)
Z	4
Data collection and refinement	
Radiation, wavelength (Å)	Mo$K\alpha$, λ = 0.71073
Temperature (K)	293
Maximum observed 2θ (°)	71.65
Measured reflections	20222
Unique reflections	3933
Reflections $F_o > 4\sigma(F_o)$	3457
R_{int} after absorption correction	0.0196
$R\sigma$	0.0137
Range of h, k, l	$-21 \le h \le 22$ $-9 \le k \le 10$ $-16 \le l \le 17$
R_1 [F_o>4 σ F_o]	0.0240
R_1 (all data)	0.0286
wR_2 (on F_o^2)	0.0702
Goodness of fit	1.065
Number of least-squares parameters	179
Maximum and minum residual peak (e/Å^3)	0.37 (at 0.69 Å from O2) -0.46 (at 0.50 Å from S)

($|E^2-1|$=0.869) agrees with the centrosymmetric nature of melanterite. The crystal structure of melanterite was refined, using SHELXL-2014 (Sheldrick, 2015), starting from the atomic coordinates given by Anderson et al. (2007). After several cycles of isotropic refinement, the R_1 factor converged to 0.078, thus indicating the correctness of the structural model. Taking into account the results of the electron microprobe analysis, the site scattering at the $M1$ and $M2$ sites was modeled using the scattering curves, taken from the International Tables for Crystallography (Wilson, 1992), of Fe *vs* Mg. At the S and all the O positions, the scattering curves of S and O were used, respectively. Although the hydrogen positions have been given in previous studies (e.g., Anderson et al., 2007), their positions were sought in the difference-Fourier maps. In order to avoid too short O-H distances, a soft restraint for these distances was applied. An anisotropic model for all the atom positions (except the H ones) converged to 0.0240 for 3457 unique reflections with F_o>4σ(F_o) and 179 refined parameters. Details of data collection and crystal structure refinement are reported in Table 1. Table 2 reports atomic coordinates, site occupancies, and isotropic or equivalent isotropic displacement parameters. Selected bond distances for cations are shown in Table 3.

DESCRIPTION OF THE CRYSTAL STRUCTURE

General features and cation coordinations

In agreement with previous works (Baur, 1964; Fronczek et al., 2001; Peterson, 2003; Anderson et al., 2007), the crystal structure of melanterite is formed by a SO_4 tetrahedron, two independent $M(H_2O)_6$ octahedra, and one interstitial H_2O group which is not directly bonded

Table 2. Atomic coordinates, site occupation factors (s.o.f.), and isotropic (*) or equivalent isotropic displacement parameters (in Å^2) for melanterite.

Site	s.o.f.	x/*a*	y/*b*	z/*c*	$U_{eq/iso*}$
*M*1	$Fe_{0.92(1)}Mg_{0.08(1)}$	0	0	0	0.02253(7)
*M*2	$Fe_{0.93(1)}Mg_{0.07(1)}$	½	0	½	0.02263(7)
S	$S_{1.00}$	0.22670(2)	0.47165(4)	0.17616(2)	0.02070(6)
O1	$O_{1.00}$	0.20482(6)	0.47065(13)	0.03726(7)	0.02934(16)
O2	$O_{1.00}$	0.13742(6)	0.53708(13)	0.21196(8)	0.03089(16)
O3	$O_{1.00}$	0.30786(6)	0.61609(14)	0.22691(8)	0.03463(18)
O4	$O_{1.00}$	0.25466(6)	0.26373(12)	0.22602(8)	0.03302(17)
Ow1	$O_{1.00}$	0.11233(8)	0.38395(18)	0.43126(10)	0.0526(3)
Ow2	$O_{1.00}$	0.10036(7)	0.95775(14)	0.18169(9)	0.03791(19)
Ow3	$O_{1.00}$	0.03025(6)	0.79316(13)	0.43223(8)	0.03415(17)
Ow4	$O_{1.00}$	0.47936(6)	0.45868(15)	0.17967(7)	0.03343(17)
Ow5	$O_{1.00}$	0.43178(7)	0.28426(14)	0.44160(8)	0.03549(18)
Ow6	$O_{1.00}$	0.35472(6)	0.85897(14)	0.44106(8)	0.03622(19)
Ow7	$O_{1.00}$	0.36367(8)	0.00531(13)	0.11505(10)	0.03607(19)
H11	$H_{1.00}$	0.1459(15)	0.259(2)	0.450(2)	0.073(6)*
H12	$H_{1.00}$	0.1183(15)	0.432(3)	0.3527(14)	0.057(5)*
H22	$H_{1.00}$	0.1235(15)	0.823(2)	0.2041(19)	0.065(6)*
H24	$H_{1.00}$	0.1549(13)	0.047(3)	0.210(2)	0.073(7)*
H31	$H_{1.00}$	0.0878(10)	0.872(3)	0.4643(16)	0.047(5)*
H32	$H_{1.00}$	-0.0163(16)	0.876(3)	0.373(2)	0.089(8)*
H43	$H_{1.00}$	0.4187(12)	0.511(3)	0.191(2)	0.061(6)*
H47	$H_{1.00}$	0.5315(13)	0.472(3)	0.2536(16)	0.059(6)*
H54	$H_{1.00}$	0.3761(12)	0.277(3)	0.3685(15)	0.067(6)*
H57	$H_{1.00}$	0.4065(19)	0.358(4)	0.502(2)	0.095(8)*
H61	$H_{1.00}$	0.3009(12)	0.922(3)	0.4612(18)	0.056(5)*
H63	$H_{1.00}$	0.3380(15)	0.776(3)	0.3693(15)	0.067(6)*
H74	$H_{1.00}$	0.3137(16)	0.084(4)	0.137(2)	0.089(8)*
H76	$H_{1.00}$	0.3359(19)	-0.122(3)	0.080(2)	0.100(9)*

Table 3. Selected bond distances (in Å) for melanterite.

*M*1	– Ow1	2.0717(9) ×2	*M*2	– Ow4	2.0984(8) ×2	S	– O3	1.4683(8)
	– Ow3	2.1321(8) ×2		– Ow5	2.1023(8) ×2		– O4	1.4726(8)
	– Ow2	2.1374(9) ×2		– Ow6	2.1745(8) ×2		– O2	1.4778(8)
							– O1	1.4808(8)
	average	2.114		average	2.125		average	1.475

to M^{2+} cations. Fourteen H-bonds occur, connecting *M*1- and *M*2-centered octahedra to the SO_4 tetrahedra, giving rise to an undulating layer showing the alternation, along **a**, of SO_4-*M*1-SO_4-*M*2 polyhedra (Figure 3).

The S atom is tetrahedrally coordinated by four oxygen atoms, with average <S–O> distance of 1.475 Å. This value agrees with the average <S–O> distance reported in melanterite by Baur (1964), i.e. 1.474 Å, and is slightly shorter than the <S-O> distance found by Fronczek et al. (2001), i.e. 1.481 Å. Moreover, it is in accord with the

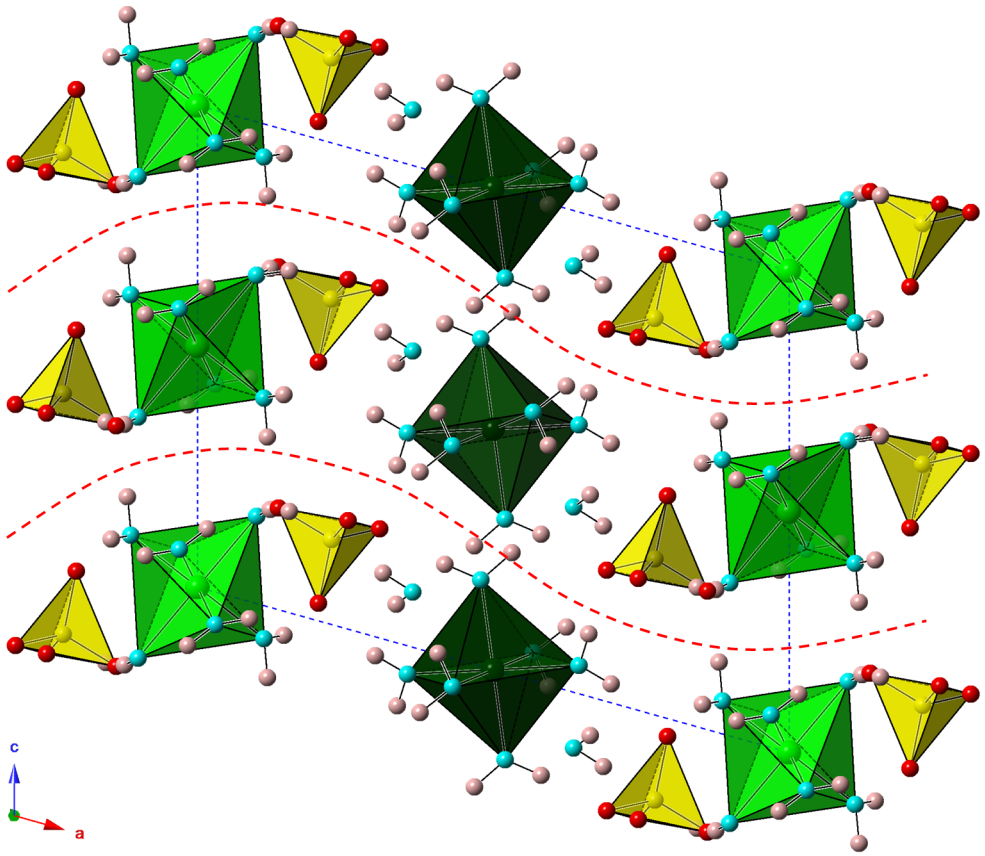

Figure 3. The crystal structure of melanterite, as seen down **b**. Symbols: light green and dark green polyhedra represent *M*1 and *M*2 sites, respectively. Yellow polyhedra represent S site. Red, light blue, and pink circles represent O, Ow, and H sites, respectively. The red dashed lines highlight the undulating layers formed by the alternation along **a** of SO_4–*M*1–SO_4–*M*2 polyhedra.

average <S-O> distance in sulfate minerals, i.e. 1.473 Å (Hawthorne et al., 2000). The corresponding bond-valence sum (BVS - Table 4), calculated on the basis of the bond parameters of Brese and O'Keeffe (1991), is 5.98 valence unit (v.u.).

Iron is octahedrally coordinated by H_2O groups both at *M*1 and *M*2 sites. The M-O bond distances range between 2.072 (*M*1-Ow1) and 2.174 Å (*M*2-Ow6), agreeing with previous structural determinations (e.g., Baur, 1964; Fronczek et al., 2001). The average <M-O> distances are 2.114 and 2.125 Å for *M*1 and *M*2 sites, respectively, slightly shorter than the ideal Fe-O distance (2.14 Å), calculated by using the ionic radii given by Shannon (1976) for $^{VI}Fe^{2+}$ (0.78 Å) and $^{III}O^{2-}$ (1.36 Å). These could be related to the minor replacement of Fe by Mg, having a smaller ionic radius (0.72 Å). Indeed, the refined site scattering at *M*1 and *M*2 confirms such a minor replacement of Fe^{2+} by Mg^{2+}, in agreement with the electron microprobe data. The refined site occupation factors (s.o.f.) at these two sites are $Fe_{0.92}Mg_{0.08}$ and $Fe_{0.93}Mg_{0.07}$. On the basis of these s.o.f., the calculated BVS at *M*1 and *M*2 are 2.12 and 2.06 v.u., respectively.

Even if some of the previous structural studies reported the distortion of the *M*2-centered polyhedron from the ideal octahedral geometry, the differences between *M*1 and *M*2 is small. In order to estimate the degree of distortion of an octahedron, different geometrical parameters can be used. According to Robinson et al. (1971), the measure of the distortion of coordination polyhedra can be expressed by using two parameters, i.e. the bond angle variance (σ^2) and the mean quadratic elongation (λ). For a coordination octahedron, the former is defined as $\sigma^2=(1/11)\Sigma(\theta_i - 90°)^2$, and the latter as $\lambda=(1/6)\Sigma(l_i-l_0)^2$, where θ_i are the bond angles, l_i are the observed bond lengths, and l_0 is the ideal bond length in an undistorted octahedron equal in volume to the one in question. The bond angle variance is slightly larger at *M*1 than at *M*2 (8.9 vs 2.20), whereas the mean quadratic elongation is 1.003 and 1.001 at *M*1 and *M*2, respectively, indicating a small distortion from the ideal octahedral geometry.

Table 4. Weighted bond-valence sums (in valence unit) in melanterite.

Site	*M*1	*M*2	S	Σv_a	Σv_a(corr)
O1			1.47	1.47	2.02
O2			1.48	1.48	2.02
O3			1.52	1.52	2.03
O4			1.51	1.51	2.00
Ow1	$0.40^{\times 2\downarrow}$			0.40	0.01
Ow2	$0.33^{\times 2\downarrow}$			0.33	-0.01
Ow3	$0.33^{\times 2\downarrow}$			0.33	0.03
Ow4		$0.37^{\times 2\downarrow}$		0.37	-0.03
Ow5		$0.36^{\times 2\downarrow}$		0.36	0.01
Ow6		$0.30^{\times 2\downarrow}$		0.30	0.06
Ow7					-0.02
Σv_c	2.12	2.06	5.98		

Note: right superscripts indicate the number of equivalent bonds involving anions. For sites with mixed occupancy, BVS have been weighted according to the proposed site population. Σv_a(corr) = BVS corrected taking into account H-bonds.

Hydrogen bonding

The examination of the BVS at the eleven independent anion positions (Table 4) reveals that all of them are underbonded. In particular, oxygen atoms at O1-O4 sites show BVS ranging between 1.47 and 1.52 v.u., whereas oxygen atoms at Ow1-Ow6 sites have BVS in the range 0.30-0.40 v.u. In addition, Ow7 is not bonded to any cation. This observation agrees with the important role played by hydrogen bonds in the crystal structure of melanterite.

The geometrical features of the H-O···H bonds are given in Table 5. The H-O···H angles range between 117 and 178°, in agreement with values given in literature (e.g., Hawthorne, 1992).

Each S-coordinated oxygen atom is acceptor of three H-bonds from H_2O groups. Taking into account the O···O distances and applying the relationship given by Ferraris and Ivaldi (1988), the corrected BVS at these oxygen atoms (O1-O4 sites) range between 2.00 and 2.03 v.u. On the contrary, the H_2O groups at Ow1-Ow5 sites are donor of H-bonds only, and their BVS, after correction, range between -0.03 and 0.01 v.u. The H_2O group hosted at the Ow6 site is both donor of two H-bonds (to O1 and O3) and acceptor from Ow7, achieving a BVS of 0.06 v.u.

Table 5. Hydrogen-bond lengths (in Å) and angles (in °) for melanterite.

Donor (D)	D–H	Acceptor (A)	H···A	D–H···A angle	<D··· A>
Ow1–H11	0.934(13)	O1	1.848	161.2	2.7493(12)
Ow1–H12	0.946(12)	O2	1.784	175.1	2.7278(12)
Ow2–H22	0.944(13)	O2	1.868	163.7	2.7875(13)
Ow2–H24	0.948(13)	O4	1.962	165.2	2.8880(13)
Ow3–H31	0.942(12)	O1	1.923	177.4	2.8644(12)
Ow3–H32	0.956(13)	O2	2.006	162.2	2.9317(12)
Ow4–H43	0.960(13)	O3	1.840	175.1	2.7973(13)
Ow4–H47	0.943(13)	Ow7	1.782	175.1	2.7226(13)
Ow5–H54	0.962(12)	O4	1.989	175.8	2.9498(12)
Ow5–H57	0.960(13)	Ow7	1.770	178.3	2.7293(13)
Ow6–H61	0.939(12)	O1	1.906	167.7	2.8309(12)
Ow6–H63	0.937(12)	O3	1.835	178.4	2.7714(11)
Ow7–H74	0.954(14)	O4	1.858	159.8	2.7734(13)
Ow7–H76	0.949(14)	O3	2.455	117.4	3.115(13)
		Ow6	2.244	139.7	3.0309(14)

The seventh H_2O group, interstitially occurring in the crystal structure of melanterite, is both donor and acceptor of H-bonds. Indeed, it is acceptor of two H-bonds from Ow4 and Ow5 and it is donor to O4 and in the bifurcated H-bond with O3 and Ow6. Its BVS is -0.02 v.u.

CONCLUSION

The crystallographic study carried out on a specimen of melanterite from Fornovolasco (Apuan Alps, Italy) allowed the first determination of the H-bond system on a natural sample. Indeed, as stated above, all the previous studies dealing with the role played by H in the crystal structure of melanterite were performed on synthetic samples, in some cases deuterated to be used for neutron powder diffraction.

The present study is a good compromise between the high-accuracy of a single-crystal X-ray diffraction in the determination of the non-H atom positions and the location of H atoms in a natural non-deuterated sample. The H-bond system determined on this natural material fully agrees with that proposed by Anderson et al. (2007) for deuterated $FeSO_4 \cdot 7D_2O$, using neutron powder data.

Since six out of the seven H_2O groups are coordinated by Fe^{2+} cations, the chemical formula of melanterite should be more correctly written as $Fe(H_2O)_6(SO_4) \cdot H_2O$.

ACKNOWLEDGEMENTS

This research received support by MIUR through the project SIR 2014 "THALMIGEN - Thallium: Mineralogy, Geochemistry, and Environmental Hazards" granted to CB (grant no. RBSI14A1CV). The University Centrum for Applied Geosciences (UCAG) is acknowledged for the access to the E.F. Stumpfl electron microprobe laboratory and Federica Zaccarini is warmly thanked for her assistance during chemical analyses. Comments by an anonymous reviewer improved the manuscript.

REFERENCES

Anderson J.L., Peterson R.C., Swainson I.P., 2007. The atomic structure and hydrogen bonding of deuterated melanterite, $FeSO_4 \cdot 7D_2O$. The Canadian Mineralogist 45, 457-469.

Baur W.H., 1964. On the crystal chemistry of salt hydrates. III. The determination of the crystal structure of $FeSO_4 \cdot 7H_2O$ (melanterite). Acta Crystallographica 17, 1167-1174.

Biagioni C., Bonaccorsi E., Orlandi P., 2011. Volaschioite, $Fe^{3+}{}_4(SO_4)O_2(OH)_6 \cdot 2H_2O$, a new mineral species from Fornovolasco, Apuan Alps, Tuscany, Italy. The Canadian Mineralogist 49, 605-614.

Brese N.E. and O'Keeffe M., 1991. Bond-valence parameters for solids. Acta Crystallographica B47, 192-197.

Bruker AXS Inc., 2004. APEX 2. Bruker Advanced X-ray Solutions, Madison, Wisconsin, USA.

Chio C.H., Sharma S.K., Muenow D.W., 2005. Micro-Raman studies of hydrous ferrous sulfates and jarosites. Spectrochimica Acta A61, 2428-2433.

D'Achiardi A., 1872. Mineralogia della Toscana. Vol. 1. Forni Editore, Pisa.

D'Orazio M., Biagioni C., Dini A., Vezzoni S., 2017. Thallium-rich pyrite ores from the Apuan Alps, Tuscany: constraints for their origin and environmental concerns. Mineralium Deposita 52, 687-707.

Ferraris G. and Ivaldi G., 1988. Bond valence vs bond length in O···O hydrogen bonds. Acta Crystallographica B44, 341-344.

Frau F., 2000. The formation-dissolution-precipitation cycle of melanterite at the abandoned pyrite mine of Genna Luas in Sardinia, Italy: environmental implications. Mineralogical Magazine 64, 995-1006.

Fronczek F.R., Collins S.N., Chan J.Y., 2001. Refinement of ferrous sulfate heptahydrate (melanterite) with low-temperature CCD data. Acta Crystallographica E57, i26-i27.

Hawthorne F.C., 1992. The role of OH and H_2O in oxide and oxysalt minerals. Zeitschrift für Kristallographie 201, 183-206.

Hawthorne F.C., Krivovichev S.V., Burns P.C., 2000. The crystal chemistry of sulfate minerals. Reviews in Mineralogy and Crystallography 40, 1-101.

Peterson R.C., 2003. The relationship between Cu content and distortion in the atomic structure of melanterite from the Richmond mine, Iron Mountain, California. The Canadian Mineralogist 41, 937-949.

Peterson R.C., Hammarstrom J.M., Seal II R.R., 2006. Alpersite $(Mg,Cu)SO_4 \cdot 7H_2O$, a new mineral of the melanterite group, and cuprian pentahydrite: their occurrence within mine waste. American Mineralogist 91, 261-269.

Robinson K., Gibbs G.V., Ribbe P.H., 1971. Quadratic elongation: a quantitative measure of distortion in coordination polyhedra. Science 171, 567-570.

Shannon R.D., 1976. Revised effective ionic radii and systematic studies of interatomic distances in halides and chalcogenides. Acta Crystallographica A32, 751-767.

Sheldrick G.M., 2015. Crystal structure refinement with SHELXL. Acta Crystallographica C71, 3-8.

Sobron P. and Alpers C.N., 2013. Raman spectroscopy of efflorescent sulfate salts from Iron Mountain mine superfund site, California. Astrobiology 13, 270-278.

Wilson A.J.C. (editor), 1992. International Tables for Crystallography Volume C: Mathematical, Physical and Chemical Tables. Kluwer Academic Publishers, Dordrecht, The Netherlands.